On the Mechanism of Gating Charge Movement of ClC-5, a Human Cl^-/H^+ Antiporter

Giovanni Zifarelli, Silvia De Stefano, Ilaria Zanardi, and Michael Pusch

Istituto di Biofisica, The National Research Council, Genoa, Italy

Supplementary Material

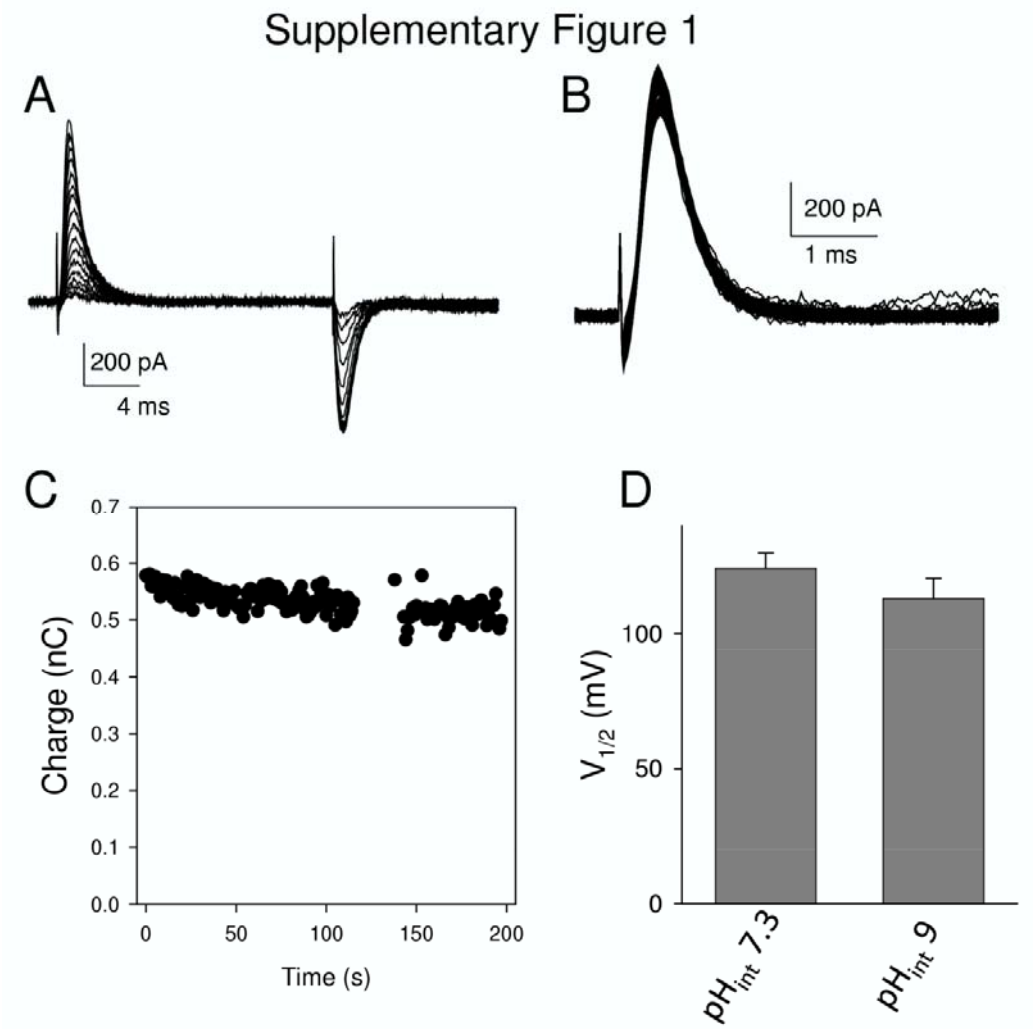

Figure S1. Intracellular protons are not needed for transient currents of E268A. Panel **A** shows currents from a transfected HEK cell evoked by voltage-steps ranging from 200 to 60 mV in -20 mV steps. The internal pH was 9 in this recording. In **B** the successive response to pulses to 200 mV are overlaid. Pulses were applied approximately once per second. Currents are from the same cell as in panel A (currents in A were acquired after these repetitive pulses). The first pulse was obtained a few seconds after the establishment of the whole cell configuration. In **C** the integral of the traces shown in B is plotted as a function of time. Note the stability of the currents despite the perfusion of the cell with a solution of pH 9. Similar results were obtained with two other cells at pH 9 and also two cells at pH 10, however, seals became unstable at pH 10 after around 30 secs. In **D** are plotted the average values of the voltage of half maximal activation obtained from Boltzmann fits to the Q(V) relationships.

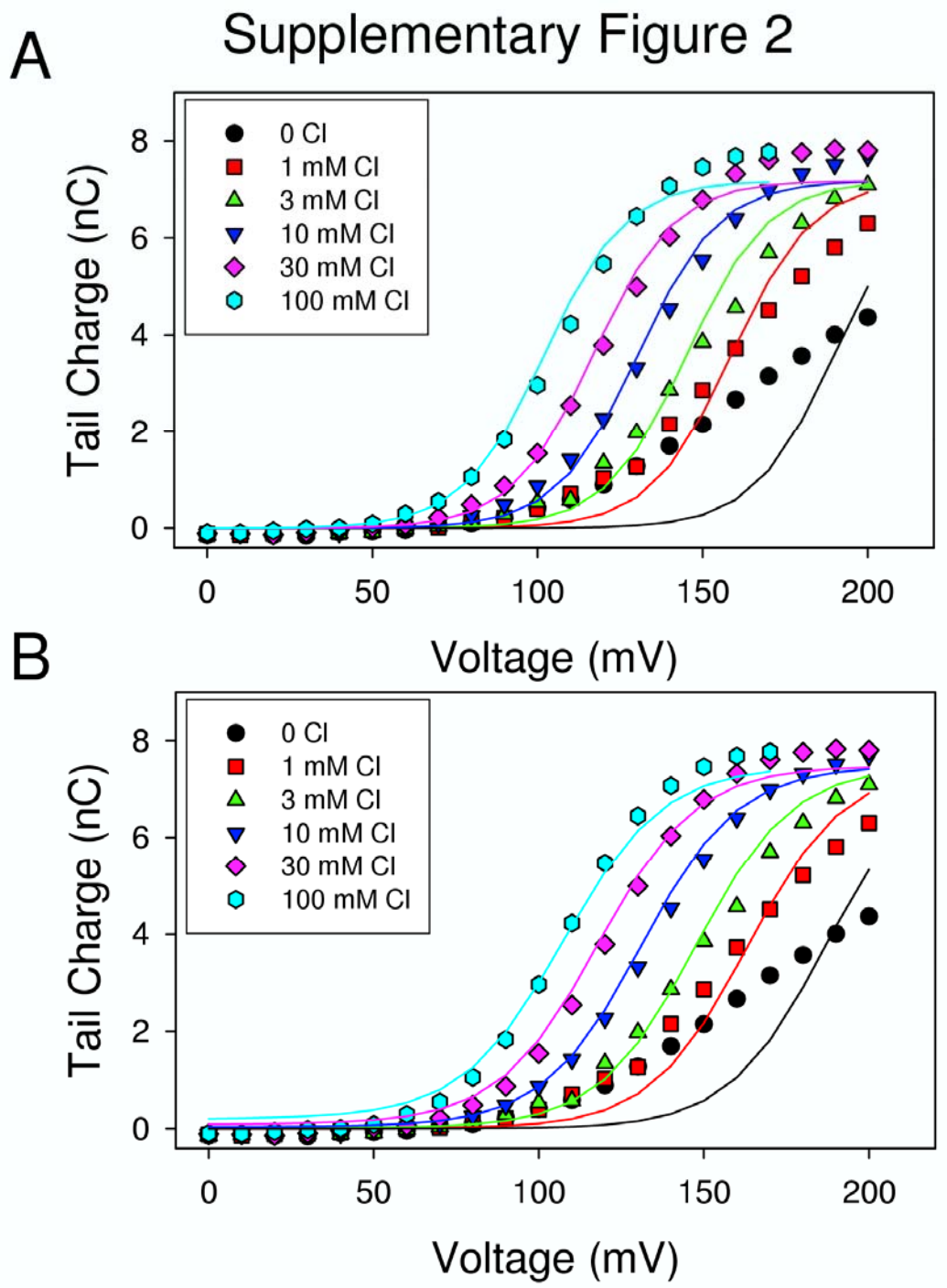

Figure S2. Models (I) and (II) fail to account for the Cl^- dependence of the transient currents.

The data points of Fig. 2E are shown superimposed with a fit of predictions of Model (I) (**A**) and Model (II) (**B**), respectively. In Model (I) state *U* represents the unbound transporter and state *B* the transporter in which Cl^- is bound with a voltage dependent dissociation constant $K_D(V)=k_{off}/k_{on}=K_D(0)exp(-z_K\varphi)$, where $\varphi = V\,F/(RT)$. Model (I) predicts a Q(V) relationship of the form

$$Q(V) = \frac{Q_{max}}{1 + \frac{K_D(0)e^{-z_K\varphi}}{[Cl]}}$$

Lines in panel **A** represent the best fit of this equation to the data points.

For Model (II) the charge voltage-relationship can be calculated by $Q(V) \sim z_K\, p(B) + (z_K + z_C)\, p(B^*)$, where $p(B)$ is the probability to be in state B and $p(B^*)$ is the probability to be in state B^*. Thus, standard equilibrium analysis yields

$$Q(V) = Q_{max} \frac{1 + \frac{z_K}{z_K + z_C} r_0 e^{-z_C\varphi}}{1 + r_0 e^{-z_C\varphi} + \frac{K_D(0) r_0 e^{-(z_C + z_K)\varphi}}{[Cl]}}$$

where $r_0 = \beta_0/\alpha_0$. *P*anel **B** shows the data points of Fig. 3E superimposed with a fit this equation. For the "0 Cl" data a contaminating concentration of 80 µM was assumed (see Fig. S3).

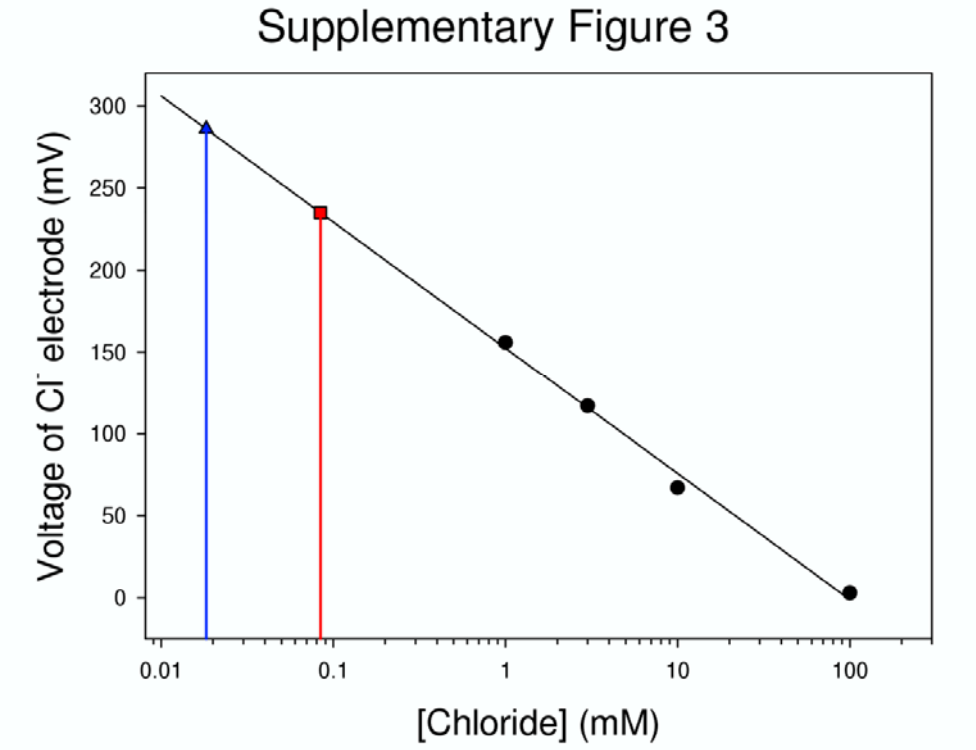

Figure S3. Residual Cl^- concentration at nominal zero chloride. Due to ubiquitous contamination, it is practically impossible to achieve a Cl^- concentration below the micromolar range. In order to estimate the residual Cl^- concentration in our nominal zero Cl^- solution, we employed a chloride-sensitive microelectrode, and measured its response to our experimental solutions. Pipettes were prepared from silanized voltage-clamp pipettes, whose tip was filled with chloride ionophore I (*meso*-Tetraphenylporphyrin manganese(III)-chloride complex) (Sigma, Milan, Italy). Pipettes were backfilled with a buffered saline and connected to a custom high impedance amplifier. A 3 M KCl filled microelectrode served as reference. For $[Cl^-]_{ext}$ >= 1 mM, the response was logarithmic with a slope of ~ 70 mV / decade. From the response to the nominal zero Cl^- solution (red square), a residual contamination of ~ 80 µM was estimated (red dashed line). Even though this value is probably an overestimation, it indicates that the residual $[Cl^-]_{ext}$ is not negligible. Addition of 1 mM $AgSO_4$ to the nominal zero Cl^- solution (blue triangle) further reduced the apparent level of Cl^- to around 20 µM (blue dashed line). Unfortunately, $AgSO_4$ could not be used to reduce the free Cl^- concentration in the experiments with oocytes (or transfected cells) because even µM concentrations of Ag^+ induced large leak currents. In conclusion, we considered the residual Cl^- concentration to be of the order of 20-80 µM.

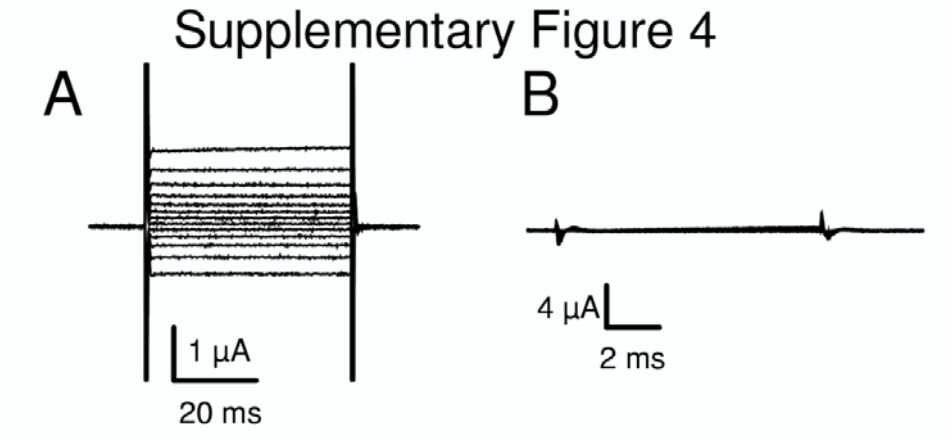

Figure S4. No transient currents are seen for mutant E211C/E268A. Panel **A** shows typical steady state Cl^- currents mediated by the E211C/E268A mutant expressed in a *Xenopus* oocyte and evoked by a pulse protocol with steps ranging from 120 mV to -20 mV. The phenotype is very similar to that of the E211A mutant. Panel **B** shows voltage clamp traces measured from the same oocyte using the same pulse protocol as used in Fig. 1 at 0 mM $[Cl^-]_{ext}$. No transient currents larger than those seen on non-injected oocytes could be observed. Very similar results were obtained in n > 4 oocytes.

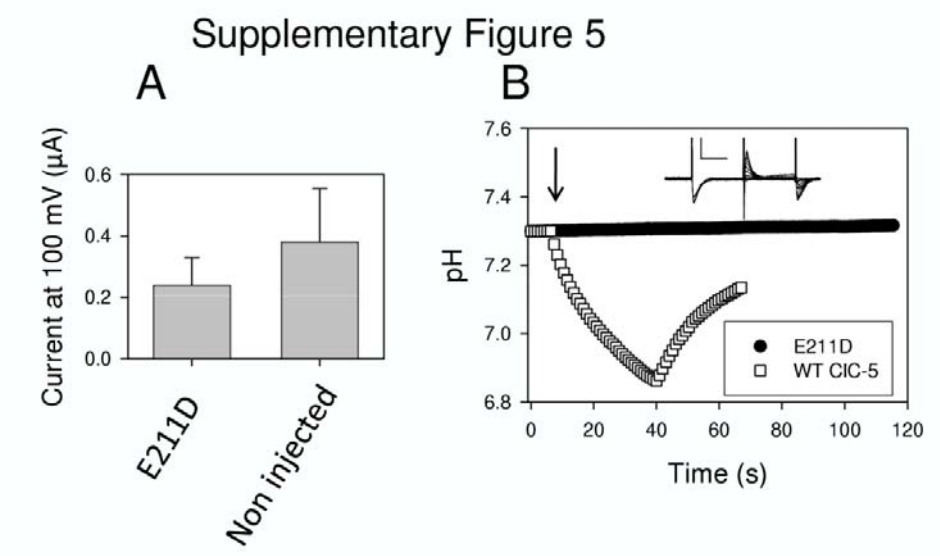

Figure S5. Mutant E211D does not show steady state transport above the level of non-injected oocytes. Panel **A** shows average steady state currents at 100 mV measured in a batch of oocytes injected with E211D or not injected. No currents above the level of non-injected oocytes are seen. In panel **B** example recordings of the extracellular pH close to the oocyte surface are shown for an E211D expressing oocyte (transient currents are shown in the inset; scale bars: 2 µA, 2 ms) and a WT ClC-5 expressing oocyte. At the time indicated by the arrow 200 ms pulses to 100 mV at 1 sec intervals were applied and led to an immediate acidification in the case of WT but not for E211D. No acidification was seen in all E211D tested oocytes (n=4).

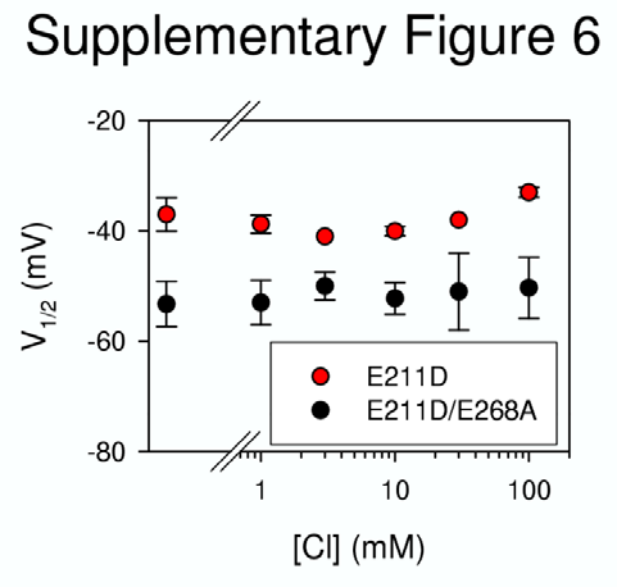

Figure S6. Transient currents of mutant E211D and E211D/E268A at pH_{ext} 7.3. Average values of $V_{1/2}$ as a function of $[Cl^-]_{ext}$ obtained by fitting the Q(V) relationship obtained for the mutants expressed in *Xenopus* oocytes with Eq. (1). Error bars indicate SEM (n>=3).

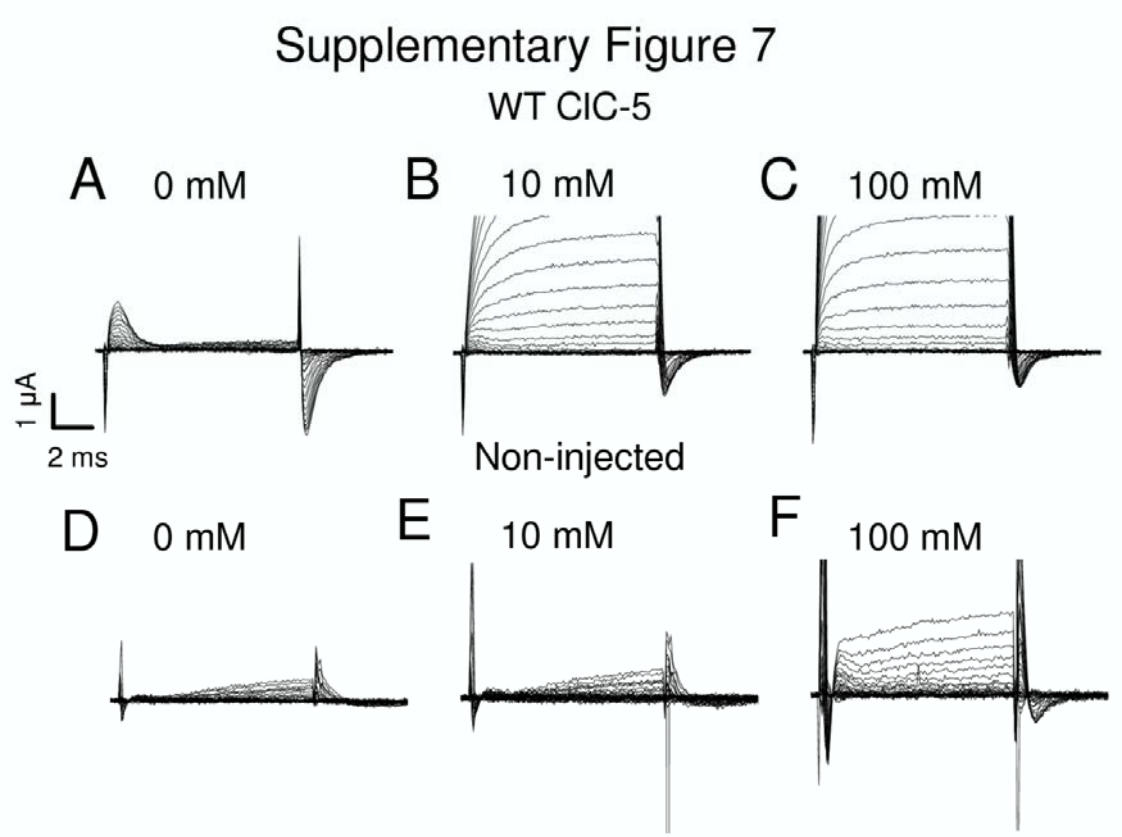

Figure S7. Comparison of transient currents seen for WT ClC-5 (upper traces) and non-injected oocytes (lower traces) at the indicated $[Cl^-]_{ext}$.